

Buneman Instability, Pierce Instability, and Double-Layer Formation in a Collisionless Plasma

S. Iizuka, K. Saeki, N. Sato, and Y. Hatta

Department of Electronic Engineering, Tohoku University, Sendai, Japan

(Received 15 May 1979)

Instabilities and double-layer formation are systematically investigated on a bounded collisionless system with electron beam penetrating through a plasma. The Buneman instability is observed at low beam currents. Above a critical current, there appears a sudden nonoscillatory potential drop due to the Pierce instability, which traps ions in the potential well. This collisionless ion trapping provides a new formation mechanism of the double layer, which is controlled by changing the speed of the potential drop.

The Buneman instability (electron-ion two-stream instability)¹ has been expected to be one of the most effective heating mechanisms in a current-carrying plasma.^{2,3} To our knowledge, however, no clear-cut experiment on this instability has been published, except our preliminary report.⁴ It is a strong convective instability, and boundary effects are quite important for experiments on the instability. There are two types of boundary: a periodic boundary and a boundary of electron-beam injection. The former corresponds to the torus experiment of Hamburger and Jancarik,⁵ in which the spectrum of fluctuations was analyzed and the anomalous resistivity was said to be attributed to the Buneman instability. The latter situation was first realized by Nezlin *et al.*⁶ They observed unstable oscillations and a virtual cathode due to the Pierce instability,⁷ although their theory is not suitable to the experiment as will be shown later. On the other hand, laminar⁸ and turbulent⁹ double layers were observed under this situation, where trapped electrons were, respectively, supplied externally and produced by the turbulent electron-electron two-stream instability. Trapped ions were also pointed out to be important for the double-layer formation. The mechanism of their initial production, however, was not explained clearly. In this Letter, we identify the Buneman instability in an electron beam-plasma system under a reasonable consideration of the boundary effect, and demonstrate a subsequent potential drop due to the Pierce instability, which provides a new mechanism of double-layer formation based on collisionless ion trapping.

The dispersion equation in an infinite plasma with beam electrons is given by

$$k^2 [1 - \omega_b^2 / (\omega - kU)^2 - \omega_i^2 / \omega^2] + k_D^2 = 0,$$

where k_D ($= \omega_e / v_e$) is the Debye wave number of plasma electrons; U and v_e are the electron-beam

speed and the thermal speed of plasma electrons, respectively; and ω_b , ω_e , and ω_i are the plasma frequencies of beam electrons, plasma electrons, and ions, respectively. Let us consider the boundary in the case of beam injection. The beam is injected at $z = 0$ and absorbed at a distance $z = L$. The dispersion equation gives four solutions for wave number k , which are coupled with each other through the boundary conditions that the fluctuations of beam density, velocity, and potential $\tilde{\phi}$ are zero at $z = 0$, and also $\tilde{\phi} = 0$ at $z = L$, as pointed out by Mikhailovskii.¹⁰ The resultant eigenfrequencies of the lowest mode (standing-wave-like mode of half wavelength) in the bounded plasma with no plasma electrons ($k_D = 0$) are calculated as shown in Fig. 1(a).

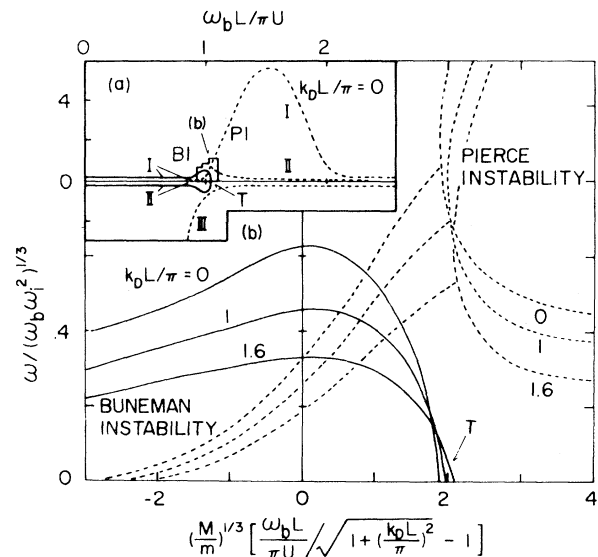


FIG. 1. Eigenfrequencies of a bounded system with electron beam penetrating through a potassium plasma. (a) Whole view for $k_D = 0$. (b) Detailed view with $k_D L / \pi$ as a parameter. Solid and dotted lines show $\text{Re}\omega$ and $\text{Im}\omega$, respectively. $\omega_b, e^2 = 4\pi n_b, e^2 / m$, $\omega_i^2 = 4\pi n_i e^2 / M$ ($n_b + n_e = n_i$).

There are three branches. For low beam densities, we find two ion plasma oscillations ($\omega = \pm \omega_i$, I and II) with quite small growth rate, and a purely damping branch (III). At a characteristic beam density ($\omega_b/U = \pi/L$), however, the former branches become highly unstable and have frequencies of $\pm 0.63(\omega_b \omega_i^2)^{1/3}$. They correspond to the Buneman instability (BI) in a bounded plasma. Above a threshold beam density shown by T in Fig. 1, two purely growing branches (I, II) and one purely damping branch (III) are excited. The branch of the largest $\text{Im}\omega$ corresponds to the nonoscillatory Pierce instability (PI) in the system of beam electrons and immovable ions ($\omega_i = 0$), which was investigated in detail by Pierce to explain the beam-current limitation.⁷ Our results yield the coupling of the Buneman instability with the Pierce instability, because ions are movable in the analysis in contrast with the works of Nezhlin *et al.*,⁶ in which these two instabilities are independent. In the presence of plasma electrons ($k_D \neq 0$), the characteristic beam density corresponding to the zero point of horizontal axis in Fig. 1(b) is given by the relation $\omega_b^2/U^2 = \pi^2/L^2 + k_D^2$. With an increase in k_D , the threshold beam density for the Pierce instability becomes large as shown in Fig. 1(b).

The experiment is performed on a synthesized collisionless plasma under a gas pressure of 5×10^{-6} Torr, as shown schematically in Fig. 2(a). A negative beam voltage $-V_b$ applied to a 6-cm-diam oxide cathode is kept in the range -5 – 0 V to prevent plasma production due to ionization. A control grid G_c is situated between a mesh anode (mesh size ≈ 2 cm) and the cathode. As the control-grid bias V_c is increased, the anode current I_a (the beam current flowing to the mesh anode) and also the beam current I_b passing through the experimental region, 10 cm long, increase linearly if there is no beam-current limitation. The beam is absorbed by a 6-cm-diam nickel plate coated with a mixture of barium oxide (BaO) and aluminosilicate ($\text{K}_2\text{O} \cdot \text{Al}_2\text{O}_3 \cdot 2\text{SiO}_2$).¹¹ The plate acts as a plasma emitter supplying a potassium plasma with temperature of about 0.15 eV and density of 10^5 – 10^8 cm^{-3} when it is heated up to 900–1100 °C. Details of this new plasma source are described elsewhere. The experimental region is also surrounded by a 6-cm-diam cylinder of nickel-chrome thin plate, the inside of which is covered with $\text{K}_2\text{O} \cdot 2\text{SiO}_2$, so as to work as a potassium-ion emitter.¹² In this work, however, ion emission from the ion emitter is used only for measurements of the

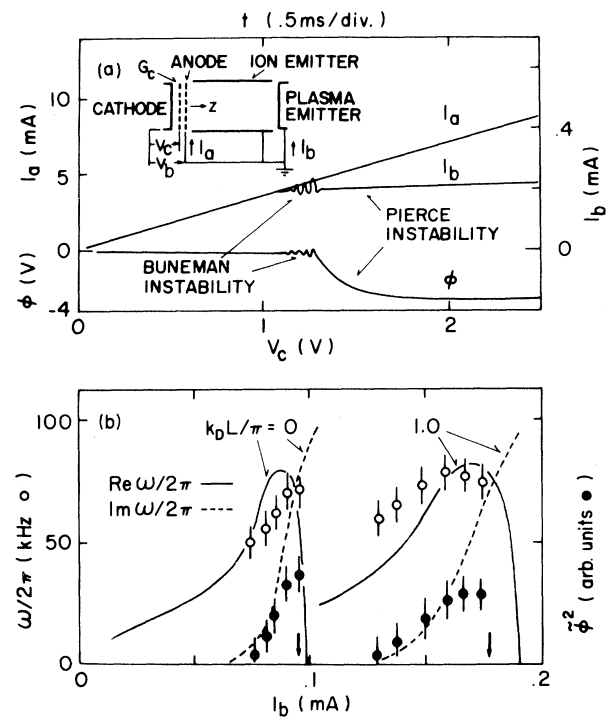


FIG. 2. (a) Instabilities for an increase of electron-beam current I_b injected into a plasma by applying a sawtooth voltage V_c to G_c at plasma density $= 5 \times 10^5$ cm^{-3} and $V_b = 3$ V. ϕ is measured at $z = 2$ cm. The apparatus is shown on the upper left side, where G_c is the control grid. (b) Frequency $\omega/2\pi$ and squared amplitude ϕ^2 of potential fluctuation due to the Buneman instability as a function of I_b , measured at $z = 5$ cm. Arrows indicate the threshold currents at which dc potential ϕ starts to drop. $V_b = 3$ V.

pure Buneman instability without stationary plasma electrons and the effects of plasma electrons on this instability [Fig. 2(b)]. The densities of beam and plasma electrons are measured by a Langmuir probe. An emissive probe is used to measure the space potential ϕ .

An intense beam injection into the plasma induces instabilities as shown in Fig. 2(a). At first, there appears an oscillation of 40–80 kHz, which is followed by a nonoscillatory potential drop. The resultant potential well of almost $-V_b$ limits the beam current I_b ,⁷ which is approximately equal to the current through the plasma emitter (the plasma-emission current is negligible). Details of the former oscillatory instability are investigated by using the ion emitter. The electron beam is injected into an ion cloud supplied from the ion emitter which is heated enough to neutralize the beam electrons. Under a low-temperature operation of the plasma emitter,

this acts only as a target and we can measure the frequency and amplitude of the *pure* Buneman instability *without plasma electrons* ($k_D = 0$). In order to clarify the plasma electron effects ($k_D \neq 0$), the plasma emitter is heated up. The oscillating potential has a standing-wave-like structure with no axial phase shift and a peak amplitude at $z = 4-6$ cm. Its phase and amplitude do not depend on the radial position [from $r = 0$ (center) to $r = 2.6$ cm]. Thus, the fluctuation is one dimensional along z . Figure 2(b) shows the observed frequency as a function of I_b . Since the linear growth rate should be proportional to the squared saturation amplitude of the instability, $\bar{\varphi}^2$,¹³ the measured values of $\bar{\varphi}^2$ are also plotted in this figure. Arrows show the threshold current at which the dc potential ϕ starts to drop. In the case $k_D L/\pi = 1$, the density ratio of plasma electrons to beam electrons n_e/n_b at the threshold current is 0.02. This result indicates a strong stabilizing effect of plasma electrons: In the presence of this small amount of plasma electrons, the threshold beam density for the potential drop is twice the threshold value at $k_D L/\pi = 0$. The data are found to be well consistent with the theoretical curves replotted from Fig. 1(b). Thus, the instability is well identified as the Buneman instability in a bounded system. The potential drop following this instability is due to the Pierce instability. The onset currents of this nonoscillatory instability are a little smaller than the predicted threshold values given by $\text{Re}\omega = 0$, probably because of the nonlinearity.

Nonlinear evolution of the nonoscillatory Pierce instability is investigated by measuring temporal changes of spatial potential distribution. A step injection of the beam into a plasma induces a sudden potential drop around $z = 2$ cm due to this instability, as shown in Fig. 3(a). Since this potential drop is much faster than the ion motion, a large amount of ions around $z = 2$ cm are trapped in the growing potential well. The bottom of the well reaches a potential nearly equal to the beam voltage $-V_b$, which reflects a part of the beam electrons and limits the beam current I_b . Figure 3(a) demonstrates that this deep potential well is deformed to result in a stationary laminar double layer in the time scale of the trapped-ion motion. Here, all ions are produced by the plasma emitter (the ion emitter is not heated). The ion trapping, however, occurs within the fast initial dropping time of the potential well which is shorter than the ion transit time of thermal motion. After the construction of the stationary double layer, the

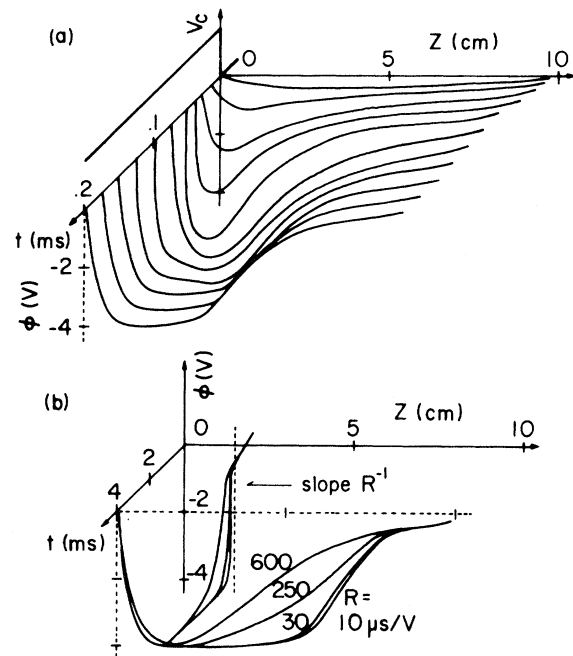


FIG. 3. (a) Double layer formation due to the Pierce instability, when a step voltage $V_c (= 10 \text{ V})$ is applied, for $V_b = 4 \text{ V}$ and $k_D L/\pi = 2.6$. (b) Control of double layer by changing the potential dropping rate R^{-1} which depends on the rise time of a ramp voltage $V_c (= 10 \text{ V})$, for $V_b = 4 \text{ V}$ and $k_D L/\pi = 3$.

plasma emitter supplies only transit ions. Thus, this double layer is one of Bernstein, Green, and Kruskal¹⁴ (BGK) solutions, which is composed of trapped electrons and transit ions from the plasma emitter, beam electrons from the cathode, and trapped ions produced by the Pierce instability. The beam electrons sustain the potential difference of the double layer to limit the beam current, and its shape is determined by shielding effects of the trapped ions and electrons. The ion trapping should be sensitive to the rate of potential drop. Figure 3(b) shows the dependence of the double layer on the rise time of ramp voltage V_c which changes the potential dropping rate R^{-1} around $z = 2$ cm. A drastic change of the potential shape is observed for $R > R_0 (= 110 \mu\text{s/V})$, where R_0 is the ion transit time divided by the potential drop $\Delta\phi = 0.15 \text{ V}$ (\approx ion thermal energy) in the initial potential well (length ≈ 2 cm). According to a computer calculation, the energy of trapped ions is just the same as the thermal energy for $R \ll R_0$. But, for $R \geq R_0$, they get an energy comparable to the potential drop (\approx the beam energy), although the amount of trapped ions is almost constant. Thus, the slope of the double-

layer potential on the low-potential side becomes gentle with an increase in R , i.e., with an increase in the Debye length of the trapped ions.

In summary, the dynamics of a bounded beam-plasma system is understood systematically. An electron-beam injection into a plasma induces the Buneman instability and the subsequent nonoscillatory Pierce instability. The sudden potential drop due to the latter instability evolves to result in the laminar double layer, because it is accompanied by collisionless ion trapping.

- ¹O. Buneman, *Phys. Rev.* **115**, 503 (1959).
²T. D. Mantei and D. Gresillon, *Phys. Rev. Lett.* **40**, 1383 (1978).
³J. S. DeGroot *et al.*, *Phys. Rev. Lett.* **38**, 1283 (1977).
⁴K. Saeki *et al.*, in *Proceedings of the Thirteenth*

International Conference on Physics of Ionized Gases, Berlin, September 1977 (Physical Society of the German Democratic Republic, Leipzig, 1977), p. 783.

- ⁵S. M. Hamberger and J. Jancarik, *Phys. Rev. Lett.* **25**, 999 (1970).
⁶M. V. Nezhlin *et al.*, *Zh. Eksp. Teor. Fiz.* **55**, 397 (1968) [*Sov. Phys. JETP*, **28**, 208 (1969)].
⁷J. R. Pierce, *J. Appl. Phys.* **15**, 721 (1944).
⁸P. Coakley *et al.*, *Phys. Rev. Lett.* **40**, 230 (1978).
⁹B. H. Quon and A. Y. Wong, *Phys. Rev. Lett.* **37**, 1393 (1976).
¹⁰A. B. Mikhailovskii, *Zh. Tekh. Fiz.* **35**, 1945 (1965) [*Sov. Phys. Tech. Phys.* **10**, 1498 (1966)].
¹¹J. P. Blewett and E. J. Jones, *Phys. Rev.* **50**, 464 (1936).
¹²N. Sato *et al.*, *Appl. Phys. Lett.* **24**, 300 (1974).
¹³L. D. Landau and E. M. Lifshitz, *Fluid Mechanics* (Pergamon, London, 1960), p. 104.
¹⁴I. B. Bernstein, J. M. Green, and M. D. Kruskal, *Phys. Rev.* **108**, 546 (1957).

Positron Annihilation Study of Defects in Succinonitrile

M. Eldrup and N. J. Pedersen

Chemistry Department, Risø National Laboratory, DK-4000 Roskilde, Denmark

and

J. N. Sherwood

Department of Pure and Applied Chemistry, University of Strathclyde, Glasgow G11XL, United Kingdom

(Received 23 July 1979)

Positron lifetime and angular correlation measurements have been made on the plastic crystal succinonitrile. They confirm the phase transition at 234 ± 1 K. In the plastic phase the average orthopositronium lifetime increases with temperature and saturates at the highest temperatures. This is interpreted as orthopositronium trapping in thermally created defects, probably vacancies. A defect formation energy of 0.36 ± 0.1 eV is deduced. This is lower than predicted values of the vacancy formation energy.

Much use has been made of the positron annihilation technique (PAT) for the examination of point defects, in particular in metals,¹ but also in ionic solids¹ and ice.² Although the technique has been applied to a number of organic molecular crystals^{3,4} it has only recently been attempted to obtain intrinsic defect properties from the results.⁵ In many molecular crystals a fraction of the injected positrons will form positronium (Ps). It is possible that this species may become localized in regions of lower than average electron density. Thus Ps may act as a probe for vacancies and vacancy clusters in these solids as do positrons in metals. If so, this would open the way for detailed studies of the formation and migration energies of such defects to supplement

the rather sparse existing information⁶ and to aid in the elucidation of self-diffusion mechanisms.⁶ In this Letter we report on positron lifetime and angular correlation measurements in the *plastic crystal*⁷ succinonitrile, $\text{CNCH}_2\text{CH}_2\text{CN}$ (SN). This material has a low-temperature brittle monoclinic phase (II) which at⁸ 233 K transforms into the plastic body-centered-cubic phase⁶ (I) with a simultaneous decrease in density. A close similarity is found between the temperature dependence of ortho-Ps lifetimes in the high-temperature plastic phase of this material and that for positrons which are being trapped in thermally created vacancies in metals.

For the lifetime measurements, high-purity (<1-ppm total impurity) melt grown SN monocrys-